RESEARCH ARTICLE | FEBRUARY 05 2019

Injection molding with time modulation of mold surface temperature. Analysis and modeling of pressure and temperature evolutions FREE

V. Speranza ✉; S. Liparoti; R. Pantani; G. Titomanlio

AIP Conf. Proc. 2065, 020002 (2019)
https://doi.org/10.1063/1.5088252

Injection molding with time modulation of mold surface temperature. Analysis and modeling of pressure and temperature evolutions

V. Speranza[1,a)], S. Liparoti[1)], R. Pantani[1)], and G. Titomanlio[1)]

[1]*Department of Industrial Engineering, University of of Salerno, via Giovanni Paolo II, 132 – 84084 – Fisciano (SA) – Italy*

[a] Corresponding author: vsperanza@unisa.it

Injection molded samples were obtained by a fast evolution of cavity surface temperature system. This technique allows to keep, for assigned time intervals, the cavity surface temperature at intermediate values between injection and cooling channels temperatures. The surface temperature was changed by activating thin heating devices layered below the cavity surface; the devices were activated by the injection molding machine at the starting of screw movement and thus the cavity surface is already heated at the contact with the polymer. The surface temperature reached a plateau after very short time and the small thickness of the heating device allowed a fast cooling at the heater deactivation.

Several tests were performed for different levels of the heating powers and heating times. The recorded evolutions of surface temperature and of pressure inside the cavity show that, for high heating power and long heating times, the pressure undergoes two pressure steps down: the first as consequence of the cooling from the injection temperature to the heated surface temperature and the second determined by the cooling to the mold temperature due to the heating deactivation. For small heating times the two cooling steps collapse into a single one.

The effects of temperature, pressure and flow on relaxation times, nucleation density, spherulitic growth rate, as well as the interrelation among these quantities were experimentally analyzed and included into an overall injection molding simulation model for the iPP grade developed in the UNISA code. The UNISA code was modified to the purpose of accounting of the surface heating. The simulation results favorably compare with the experimental results of temperature evolutions. Also, simulation results of pressure evolutions reproduce main features shown by the experimental results.

INTRODUCTION

The injection molding process has been extensively studied and optimized over the years. Its applications have become wider and wider because of its high productivity. The process is carried out with low mold temperatures, which usually are well below the polymer solidification temperature, in order to keep short the processing time and improve the productivity [1].

The increasing interest toward miniaturization [2,3] and the necessity to produce micro and nanostructured surfaces by the injection molding process [4,5] has given rise to the need to carry out the process with high mold temperatures, keeping small the increase of the processing time. In these cases, the main challenge is to perform each stage of the injection molding process with different temperature of the mold or the cavity. In particular, it could be significant to run the filling with high cavity surface temperature and the cooling stage with cavity surface temperatures below the polymer solidification temperature. Different strategies were proposed in the literature, such as proximity heating [6], induction heating [7,8], but these techniques require additional design and tool costs. Furthermore, in these techniques both the heating and the cooling rates are slow, if compared with the time of the other stages, and, as consequence, the whole processing time becomes significantly longer than the processing time of the conventional injection molding process.

In this work, a technique based on the electrical heating of a thin portion of the mold below the cavity surface was adopted. Such a technique is more versatile and does not imply a significant increase of the processing time [2,9]. In particular, a thin heater, few tenth of a millimeters, made of carbon black loaded poly(amide-imide) [10], was designed and adopted to increase the cavity temperature during the filling and the packing. The heating rate, which increases with the supplied electrical power, allows reaching the selected temperature in the time range between the mold closing and the polymer entering into the cavity. The heater reduced thickness allows a fast cooling after the heater deactivation [11]. Experimental results of temperature evolutions are discussed and compared with simulation results.

Proceedings of PPS-34
AIP Conf. Proc. 2065, 020002-1–020002-6; https://doi.org/10.1063/1.5088252
Published by AIP Publishing. 978-0-7354-1793-9/$30.00

EXPERIMENTAL

The polypropylene (i-PP) grade adopted in this study was supplied by Montell (now Basell), and its commercial name is T30G (non-nucleated, Mw=376 000, Mw/Mn=6.7, tacticity=87.6%): it was extensively characterized as far as rheology and crystallization kinetics [8-12]. The device used to control the cavity surface temperature evolution was well described elsewhere [13].

A 70-ton Negri-Bossi reciprocating screw injection molding machine was used for the experiments. The polymer was injected into a line gated rectangular cavity having length L=110 mm, width W=12.7 mm, and thicknesses S=1.5 mm. Figure 1 shows the cavity adopted for the injection experiments. The molding machine and the mold were equipped with five pressure transducers distributed along the flow path: one in the injection chamber (P0), one just before the gate (P1) and three in the cavity (P2, P3 and P4), located in the non-moving part of the mold (15 mm, 60 mm and 105 mm downstream from the gate position). Moreover, a temperature sensor was located in the cavity in positions P2. Heating devices were located on both sides of the cavity. The injection molding experiments were carried out adopting 3.7 s injection time (flow rate 2.3 cm^3s^{-1}), 220°C melt temperature, 25°C mold temperature, 72 MPa packing pressure, and 8 s holding time. The fast evolution of the cavity surface temperature was obtained by ohmic heating, supplying 9.5 W/cm^2 electrical power to each heating device (that gives rise to 150°C asymptotic cavity surface temperature), with heating times of 1.3 s, 6 s, 12 s and 20 s. The heating devices were activated two seconds before the melt reached the position P2. The heating element was a 50 μm poly(amide-imide) loaded carbon black film, layered below the cavity surface [12]. It was electrically insulated from the mold by two poly(amide-imide) layers, 20 μm thickness, and an additional layer of 120 μm thickness was located on the mold side, to reduce the heat loss toward the mold. A protective steel layer (0.1 mm thickness) covering all the length of the cavity was adopted to avoid the direct contact of the melt with the heating device.

TABLE 1 summarizes all the adopted operating conditions. The name of each test is composed by the asymptotic temperature (T_{level}, measured on the protective steel layer), the heating time t_h and the holding pressure, P_{hold}, 72 MPa for the tests reported in this work. The Passive-72 experiment was obtained without activating the heating devices and the Steel-72 replacing the heating devices with steel layers of equal thickness.

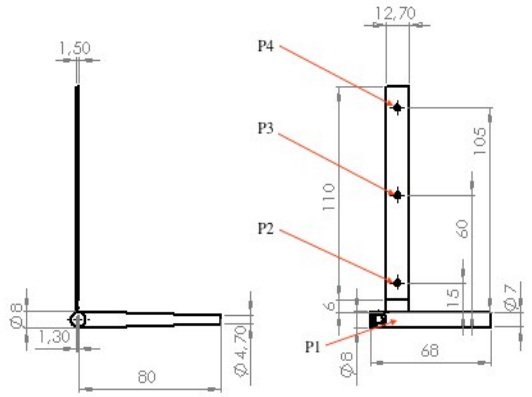

FIGURE 1 Geometry of the cavity (P1-P4 indicate the pressure transducers positions).

Test run	P_w (W/cm^2)	T_{level} (°C)	t_h (s)	P_{hold} (MPa)
Steel-72	0	28	0	72
Passive-72	0	28	0	72
150-1.3-72	9.5	150	1.3	72
150-6-72	9.5	150	6	72
150-12-72	9.5	150	12	72
150-20-72	9.5	150	20	72

TABLE 1 Operating conditions adopted for the injection molding experiments. (P_w=electrical power applied; T_{level}= temperature reached on the steel layer; t_h=time that the heater is activated after the polymer reaches position P2; P_{hold}=holding pressure).

RESULTS

The temperature recordings obtained in position P2 for all tests reported in TABLE 1 are reported in Figure 2. During the 2 s of heating before the contact with the polymer, the cavity surface reaches a temperature close to its asymptote, which is reached after about 5 s of additional heating time. At the first contact with the hot melt, the surface temperature undertakes a jump of about 60°C and then it immediately starts to decrease toward the asymptote. The surface temperature decreases, at the heater deactivation, with a cooling rate of about 30°C/s (and it reaches 80°C within about 4 s after the heater deactivation); afterwards, the cooling rate gradually decreases as consequence of the driving force decrease, and also by the effect of the heat of crystallization release.

The pressure evolutions recorded along the flow path in the positions P0, P1, P2, P3 and P4 with 6 s and 20 s heating times, are reported in Figure 3a and 3b, respectively. After the filling, the pressure was kept constant in position P0 for 8 s, this corresponds to the holding stage. During the gate sealing (which takes place soon after 7s for both the selected heating times), pressure in position P1 undergoes a small increase, at the same time, the pressure difference across the gate increases faster [13] and, as a consequence, the pressure P2 in the cavity starts

a faster decrease. With the longest heating times (20 s) the pressure undergoes toward two steps down: the first step takes place due to the cooling from the melt temperature to T_{level}, the second step is due to the cooling toward the temperature of the whole mold (25°C) and it takes place at the heater deactivation. If the cavity surface heating time is smaller than the gate sealing time (as in the case of Figure 3a) only one pressure step is observed.

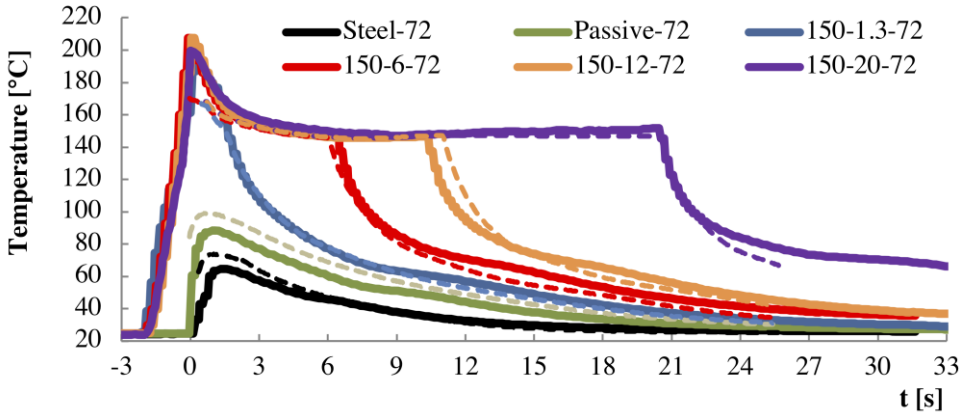

FIGURE 2 Experimental (solid lines) and simulated (dotted lines) temperature evolutions in pos. P2 for the experiment performed with 150°C cavity surface temperature and different heating times. The Steel-72 and Passive-72 tests are also reported.

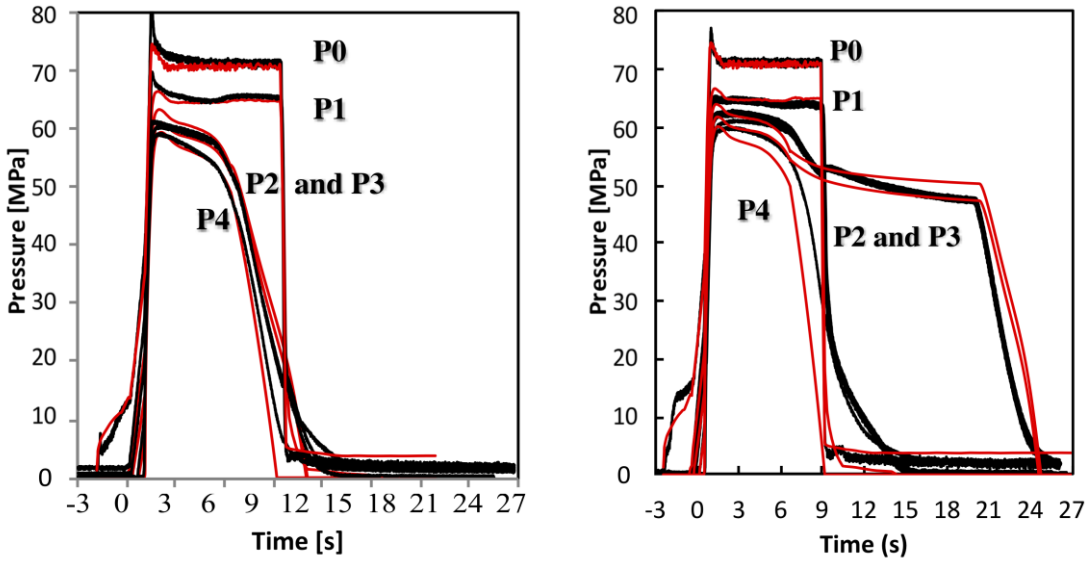

FIGURE 3 Experimental (black lines) and simulated (red lines) pressure evolutions in different positions along the flow path of the experiments 150-6-72 (a) and 150-20-72 (b).

PROCESS SIMULATION

The effects of temperature, pressure and flow on relaxation times, nucleation density, spherulitic growth rate, as well as the interrelation among these quantities and the distributions of deformation rate and cooling time during the process have to be taken into account for the process simulation. Each of the effects mentioned above was experimentally analyzed and described by a model for the iPP grade considered in this work. The combination of all these specific models became a model for polymer processing and its application to the injection molding process was implemented into the UNISA code. In particular, the crystallization kinetics toward the mesomorphic phase was described by the Nakamura equation. The Kolmogoroff equation was adopted to describe the crystallization kinetics of the α-phase, the Hoffman-Lauritzen equation describing the growth rate, with the crystallization temperature T_m function of both pressure and molecular stretch Δ. The molecular stretch, Δ, was evaluated as the difference between the two main eigenvalues of the molecular conformation tensor $\underline{\underline{A}}$ defined as

$$\underline{\underline{A}} = 3\,\frac{\left(\langle \underline{R}\underline{R}\rangle - \langle \underline{R}\underline{R}\rangle_0\right)}{\langle R_0^2\rangle}$$

where R represents the end distance of the subchain. The evolution of the conformation tensor was described by a controvariant Maxwell-type equation:

$$\frac{D}{Dt}\underline{\underline{A}} - (\underline{\nabla}\,\underline{v})^T \times \underline{\underline{A}} - \underline{\underline{A}} \times (\underline{\nabla}\,\underline{v}) = -\frac{1}{\lambda}\underline{\underline{A}} + (\underline{\nabla}\,\underline{v})^T + (\underline{\nabla}\,\underline{v})$$

where $\underline{v}$ is the velocity vector and λ represents the dominant relaxation time that, when the intensity of the flow field increases, decreases according to a Cross-type equation $\lambda = \frac{\lambda_0}{1+(a\Delta)^b}$ where a and b are material parameters.

Under simple shear, the parameter Δ is:

$$\Delta = \sqrt{A_{11}^2 + 4A_{12}^2}$$

Experimental correlations were identified between nucleation rate and the excess of the growth rate with respect to its quiescent values and for the effect of crystallinity on viscosity. Further details on the model implemented in the UNISA code and values of the parameters adopted in the constitutive equations are reported elsewhere {Formatting Citation}. The UNISA code was adapted to take into account the evolution of the cavity surface temperature. In particular, the heating device and the protective steel layer, were accounted for in the simulation by a multilayer composed by four films. The films from the cavity surface toward the mold are: the steel layer, having the same thermal conductibility of the mold, and the heating device composed by three layers, all having the thermal conductivity of the Kapton®. The generation term determined by the activation of the heating element made of carbon black loaded poly(amide-imide) was accounted for in the simulation. The heating device was thermally correlated to the mold by a heat transfer coefficient of 2950 W m^{-2} K^{-1}

COMPARISON

The results of the simulation reproduce main features of the experimental results reported above. In particular, the simulation results for the evolution of the temperatures (dotted lines in Figure 2) reproduce behavior of the experimental temperature evolution (including the second cooling).

The comparison among experimental and simulated results for the pressure evolutions is shown, for the complete test duration and in the five positions (P0-P4) where the transducers are located, in Figure 3 a and 3b for heating times 6 s and 20 s respectively. The fact that, inside the cavity in positions P2 and P3, for long heating times (larger than the gate sealing time), there are two cooling pressure steps and that, vice versa, for surface heating times smaller than the gate sealing time the two cooling steps collapse into a single larger step is clearly reproduced by the simulation. The overall comparison shows that main features of the evolutions of all pressure curves reported in the five positions (P0-P4), included the height of each cooling step, are nicely reproduced. The simulation results can thus be accredited of good reliability, at least qualitatively.

Simulation results for the evolution of crystallinity at several distances from the surface in position P2, reported in Figure 4 show that the crystallinity reaches small steady values during filling, which range from about 2% ÷ 3% at about 80 μm from the wall down to negligible values soon on the remaining part of the cross section. These values remain unchanged during the subsequent time interval (about 20 s for the test considered in Figure 4) when the wall temperature is held at T_{level} of 150°C; the crystallization proceeds and develops only during the second cooling from T_{level} to the mold temperature; the morphology is determined by the stretch distribution on the cross section at the beginning of the second cooling step.

At gate sealing, which takes place close to 7 s, the packing flow disappears. Consequently, the relaxation time recovers its quiescent value, which at 150°C is larger than 100 s and, thus, the stretch distribution remains essentially unchanged. According to the simulation, at the gate sealing time, if smaller than the heating time, the stretch distribution is completely below the threshold needed to obtain fibrillary structures; just one second before, the threshold is overcome only on a small layer 60 μm thick close to the cavity surface

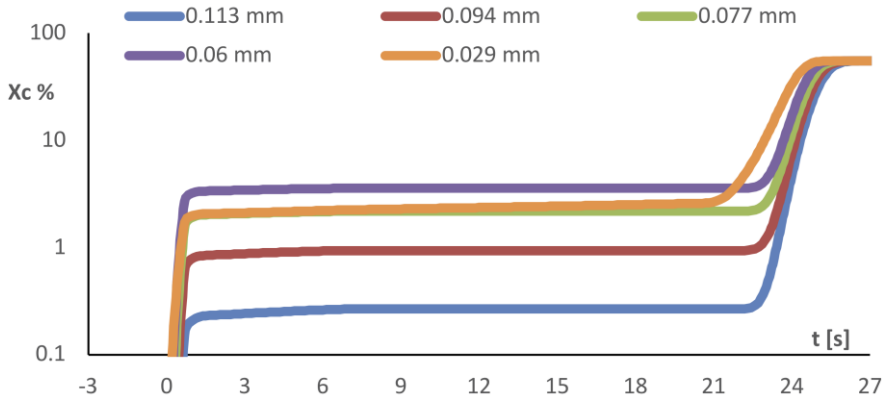

FIGURE 4 Results of the simulation for crystallinity evolutions in position P2 during the test 150-20-72

CONCLUSIONS

Injection molding tests with fast evolution of cavity surface temperature have been performed. The cavity surface temperature has been held, by electrical heating and for selected times, at a level intermediate between the injection temperature and the temperature of the mold cooling channels.

The cavity surface heating time can be modulated, depending upon the chosen objective which can be simply the reduction of the filling pressure or the control of the morphology inside the moldings.

Temperature at the cavity surface and pressures inside the cavity were recorded during the process. When the surface heating time is held larger than the gate sealing time, the pressure recordings show two cooling steps: the first corresponding to the cooling from the injection temperature to the heated cavity surface temperature and the second determined by the cooling from the heated surface temperature to the mold temperature.

The process simulation of all experimental tests has been performed by the UNISA code, suitably modified for accounting of the cavity surface heating during the process. Main features of temperature and pressure recordings where reproduced by the simulation. The simulation results can thus be accredited of good reliability, at least qualitatively. First prediction of the simulation is that within the first 6s of heating time of cavity surface at 150°C, the molecular stretch decreases to negligible values on about 90% of the sample cross section, where crystallinity is and remains, until the second cooling, negligible. This implies that, after that heating time, the polymer crystallization takes place during the cooling from the heated surface temperature T_{level} to the mold temperature and, furthermore, the stretch values are not sufficient to generate a shear layer, nowhere on the sample cross section. Vice versa the simulation results predict that a thin shear layer of about 50 μm forms at the cavity surface if the heating time is 6 s.

REFERENCES

1 D. V. Rosato, D. V. Rosato, M. V. Rosato, Plastic Product Material and Process Selection Handbook, 2004.

2 F. De Santis, R. Pantani, *Journal of Materials Processing Technology. 237 1–11 (2016)*.

3 B. Sha, S. Dimov, C. Griffiths, M.S. Packianather, *Journal of Materials Processing Technology. 183 284–296 (2007)*.

4 V. Speranza, S. Liparoti, M. Calaon, G. Tosello, R. Pantani, G. Titomanlio, *Materials and Design. 133 (2017)*.

5 M. Calaon, G. Tosello, H.N. Hansen, J. Noregaard, Influence of process parameters on edge replication quality of lab-on-a-chip micro fluidic systems geometries, in: Annual Technical Conference - ANTEC, Conference Proceedings, 2013: pp. 1084–1088. http://www.scopus.com/inward/record.url?eid=2-s2.0-84903544048&partnerID=tZOtx3y1.

6 D. Yao, T.E. Kimerling, B. Kim, *Polymer Engineering & Science. 46 938–945 (2006)*.

7 S.-C. Chen, Y.-W. Lin, R.-D. Chien, H.-M. Li, *Advances in Polymer Technology. 27 224–232 (2008)*.

8 H.L. Lin, S.C. Chen, M.C. Jeng, P.S. Minh, J.A. Chang, J.R. Hwang, *International Communications in Heat and Mass Transfer. 39 514–522 (2012)*.

9 K.M.B. Jansen, A.A.M. Flaman, *Polymer Engineering and Science. 34 898–904 (1994)*.

10 S. Liparoti, G. Landi, A. Sorrentino, V. Speranza, M. Cakmak, H.C. Neitzert, *Advanced Electronic Materials. 2 (2016)*.

11 S. Liparoti, A. Sorrentino, G. Titomanlio, *RSC Adv. 6 99274–99281 (2016)*.

12 S. Liparoti, G. Landi, A. Sorrentino, V. Speranza, M. Cakmak, H.C. Neitzert, *Advanced Electronic*

Materials. *2 1600126 (2016)*.
13 S. Liparoti, A. Sorrentino, G. Titomanlio, *Materials and Manufacturing Processes*, DOI: 10.1080/10426914.2018.1512120 *(2018)*.
14 R. Pantani, V. Speranza, G. Titomanlio, *International Polymer Processing*, 31(5), 655–663 (2016)
15 R. Pantani, V. Speranza, G. Titomanlio, *European Polymer Journal*. 97, 220–229 (2017)
16 R. Pantani, V. Speranza, G. Titomanlio, *International Polymer Processing*, 33(3), 355–362 (2018)
17 R. Pantani, F. De Santis, V. Speranza, G. Titomanlio, *AIP Conf Proc PPS-29*, 1593, 636–640 (2014)